Pacific Northwest
NATIONAL LABORATORY

PNNL-33729

Pore-Scale Simulation of Spectral Induced Polarization

December 2022

Frederick D. Day-Lewis
Timothy C. Johnson

U.S. DEPARTMENT OF ENERGY

Prepared for the U.S. Department of Energy
under Contract DE-AC05-76RL01830

DISCLAIMER

PACIFIC NORTHWEST NATIONAL LABORATORY
operated by
BATTELLE
for the
UNITED STATES DEPARTMENT OF ENERGY
under Contract DE-AC05-76RL01830

Printed in the United States of America

Available to DOE and DOE contractors from the Office of Scientific and Technical Information,
P.O. Box 62, Oak Ridge, TN 37831-0062
www.osti.gov
ph: (865) 576-8401
fax: (865) 576-5728
email: reports@osti.gov

Available to the public from the National Technical Information Service
5301 Shawnee Rd., Alexandria, VA 22312
ph: (800) 553-NTIS (6847)
or (703) 605-6000
email: info@ntis.gov
Online ordering: http://www.ntis.gov

PNNL-33729

Pore-Scale Simulation of Spectral Induced Polarization

December 2022

Frederick D. Day-Lewis
Timothy C. Johnson

Prepared for
the U.S. Department of Energy
under Contract DE-AC05-76RL01830

Pacific Northwest National Laboratory
Richland, Washington 99354

Abstract

A new model was developed to simulate spectral induced polarization (SIP) in porous media. The model is based on a pore-network approximation of the soil or rock, in which bonds between pores are represented by equivalent circuits. In the circuit model, electrolytic and surface conduction occur in parallel, with the electrolyte behaving as a single resistor, and the mineral surface behaving as a resistor and capacitor in series. Based on the pore geometry, fluid conductivity, and mineral surface conductivity, an impedance network is generated. SIP spectra are calculated by solving the sinusoidal steady-state electrical problem for a range of frequencies. The new model provides a tool to bridge the gap between (1) our fundamental understanding of polarization processes at the scale of a single pore or grains and (2) existing simulation capabilities for macroscale systems that do not account for pore-scale properties. The model is implemented in Matlab and can solve two-dimensional and three-dimensional (2D and 3D) networks. Examples for regular cubic lattices are presented, but the method and code are flexible with respect to pore geometries and allow for future leveraging of existing open-source capabilities for generation of pore networks and extraction of network geometries from micro imaging of core samples.

Acknowledgments

This research was supported by the Energy and Environment Directorate (EED) Mission Seed, under the Laboratory Directed Research and Development (LDRD) Program at Pacific Northwest National Laboratory (PNNL). PNNL is a multi-program national laboratory operated for the U.S. Department of Energy (DOE) by Battelle Memorial Institute under Contract No. DE-AC05-76RL01830.

Contents

Figures

Tables

1.0 Introduction

Spectral induced polarization (SIP) is an electrical geophysical method with potential to improve characterization and monitoring of diverse hydrologic, geochemical, and biological processes in porous media (Kemna et al., 2012). SIP spectra are sensitive to the architecture of the pore space and electrical properties of the fluid/mineral interface, which has driven increasing interest in the method for understanding processes ranging from dual-domain behavior, also known as back diffusion (e.g., Swanson et al., 2015) to detection of per- and polyfluoroalkyl substances (PFAS) (e.g., Falzone et al., 2020) to permeability estimation (e.g., Robinson et al., 2018). At the pore or grain scale, the electrical polarization mechanisms underlying SIP have been studied in the context of electrochemistry (e.g., Leroy and Revil, 1998; Lesmes and Frye, 2001) and simulated rigorously using numerical models of coupled electrochemical processes (Bucker et al., 2019). At the macro-scale, numerous equivalent circuit models (e.g., the Cole-Cole, multi-Cole-Cole and Pelton-Debye) models (e.g., Dias, 2000), have been developed; however, there are few studies where SIP measurements at the macro-scale are rigorously simulated using models that consider pore-scale characteristics. Rigorous numerical modeling of SIP mechanisms (Bucket et al., 2019) at the meso or macroscale is not tractable on existing computers; hence there is a need for computationally efficient models that can simulate polarization in model domains of scales for which measurements are possible, i.e., core size or larger. Here, we develop a new pore-network model to simulate SIP spectra to bridge the gap between micro-scale understanding and macro-scale observations.

Pore network models have been used extensively in petrophysics and digital rock physics to understand scaling behavior of physical properties and identify and understand relations between field-scale measurements and micro-scale properties of interest including porosity, pore size distribution, permeability, thermal conductivity, diffusivity, and specific surface area (Blunt, 2010). Applications to electrical geophysical problems date back to the pioneering work of Greenberg and Brace (1969), with other seminal contributions including work to relate electrical and hydraulic properties (Bernabe et al., 1995, 2010, 2011). Recently, Maineult (2017) developed a 2D pore network model for SIP and used the model to relate SIP parameters to unsaturated flow (Maineult et al., 2018). Here, we follow a similar approach but allow for 3D networks and arbitrary network geometries to consider realistic and complex porous media; this will allow for leveraging of existing open-source tools for stochastic network generation (Gostick et al., 2016) or network extraction from micro-imaging (Gostick et al., 2019). There are additional minor differences in the implementation of the pore-bond circuit model, as discussed in subsequent sections.

2.0 Background

The experimental measurement of induced polarization (IP) involves application of a low-frequency alternating current between two electrodes in contact with a rock or soil sample and measurement of the resulting sinusoidal voltage between two other electrodes. In frequency-domain IP measurements, the voltage sinusoid is characterized by magnitude and phase relative to the applied current, which can alternatively be quantified as real and imaginary resistivity (or conductivity, its inverse) (Figure 1). SIP is the collection of IP measurements over a range of frequencies (e.g., 1 mHz to 20 kHz). Effectively, SIP provides a measurement of impedance. The standard geophysical measurement process (4-electrode measurements) differs from electrical impedance spectroscopy (2-electrode measurements) commonly used in other fields. Laboratory and field SIP measurements are possible, although the former are far more common. Collection of measurements involving many combinations of electrodes allows for tomographic imaging (Kemna et al., 2012), producing images of magnitude and phase or real and imaginary conductivity.

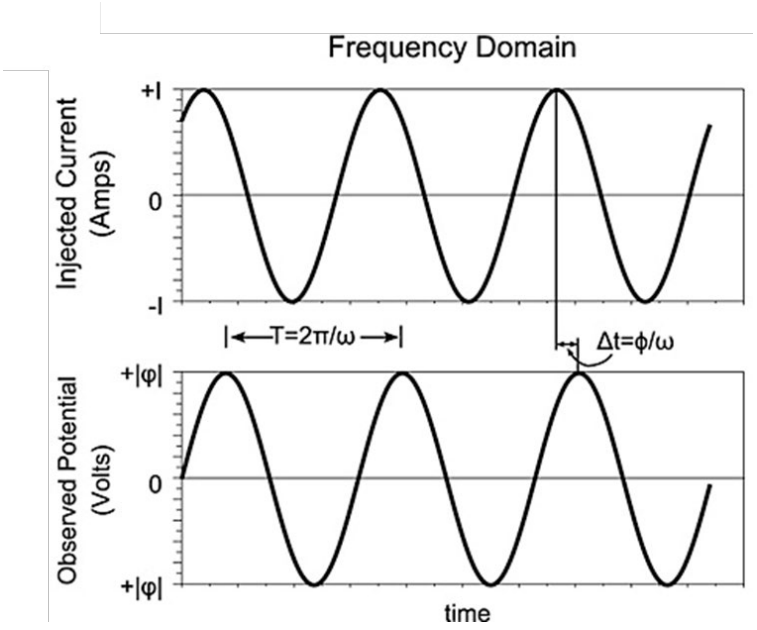

Figure 1. Schematic illustrating the basic IP measurement involving injection of an alternating current and observation of voltage, which lags the current as a result of polarization. SIP is measured by sweeping over a range of angular frequencies, ω (from Singha et al., 2015), and recording amplitude and phase spectra as a function of frequency.

At the macroscale, low-frequency electrical polarization of earth materials is commonly described using equivalent circuit models such as the widely used Cole-Cole model (Pelton, 1977), along with many other models and their respective variations (Dias, 2000). These models consist of resistor-capacitor circuits with various combinations of circuit elements in parallel and (or) series representing conduction through the fluid, conduction along grain surfaces, and different charge-storage mechanisms (e.g., Stern layer, electrical double layer, and/or membrane polarization). For example, in the Debye-Pelton (Pelton, 1977) (Figure 2), conduction occurs along parallel pathways for the fluid and the mineral surface. Electrolytic conduction in the fluid is modeled with a single resistor based on fluid conductivity, whereas conduction along the surface is modeled with a resistor and capacitor in series; hence the charge storage is associated only with the fluid/grain boundary.

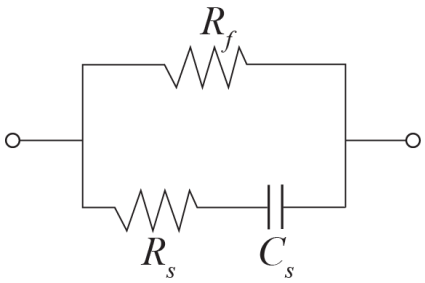

Figure 2. Debye-Pelton equivalent circuit model with parallel fluid (Rf) and surface pathways, with the resistance of the electrolytic conduction represented by a resistor (Rf), and the resistance of the surface represented by a resistor (Rs) and capacitor (Cs) in series.

Applied at the macroscale, the Debye-Pelton model is commonly formulated in terms of complex-valued bulk resistivity (Dias, 2000):

$$\rho = \rho_0 \left(1 - m\left(1 - \frac{1}{1+i\omega\tau}\right)\right), \quad (1)$$

where,

ρ is the bulk resistivity;

ρ_0 is the low frequency effective bulk resistivity, dictated by the electrolytic conduction;

$m = (\rho_0 - \rho_\infty)/\rho_0$;

ρ_∞ is the high-frequency effective bulk conductivity;

τ is the relaxation time scale associated with polarization; and

ω is the angular frequency.

The Debye-Pelton model has also been used to represent AC electrical conduction at the pore scale (Leroy et al., 2008) and in earlier work using pore network modeling for SIP (Maineult et al., 2017). Here, we use the Debye-Pelton model but formulate it in terms of the impedance of bonds between pores. Of course, many other circuit models could be considered. Dias (2000) provides a detailed review of circuit models for low-frequency polarization.

3.0 Approach

Pore network modeling requires (a) a network model describing the connections between pores and the geometric properties of pores and connecting bonds, (b) pore-scale constitutive formulae to define physical parameters required for simulation, and (c) the mathematical process model and algorithm for solution. For (a), powerful open-source tools (Gostick et al., 2016) exist for the generation of complex 2D and 3D pore networks stochastically or from micro-imaging (Gostick et al., 2019). In this report, we show results for regular, cubic-lattice networks, but the codes developed in this research are flexible with respect to network geometry in most respects. Pores can have an arbitrary number of connections (i.e., coordination number), and the pattern of connections is also arbitrary. Consistent with many pore network modeling efforts (e.g., Bernabe et al., 1995; Maineult et al., 2017, 2018), the pore space comprises only bonds; i.e., the pores are simply nodes where the electrical potentials are calculated.

For (b), we adopt the Debye-Pelton equivalent circuit model and Ohm's Law for electrolytic and surface conduction. At the scale of individual pore bonds, the Debye-Pelton circuit model gives an effective impedance in terms of fluid- and surface-pathway resistances of

$$Z = \frac{(R_f - i\omega R_f R_s C_s)}{1 - i\omega(R_f + R_s)C_s}, \tag{2}$$

where,

R_f is the resistance of the fluid pathway;

R_s is the resistance of the surface pathway; and

C_s is the capacitance of the surface pathway.

The resistance associated with the fluid pathway is calculated for each bond according to Ohm's Law and the geometric characteristics of the bond. In the examples presented here, bonds are assumed to be tubes with circular cross section:

$$R_f = \frac{L}{2\pi r_p^2 \sigma_f}, \tag{3}$$

where,

σ_f is the fluid conductivity in the bond;

r_p is the radius of the bond, assumed here to be a tube; and

L is the length of the bond, assumed to be a straight line between two pores.

The resistance associated with the mineral surface is calculated for each bond according to an assumed surface conductance (Σ_s) and the geometric characteristics of the bond:

$$R_s = \frac{L}{2\pi r_p \Sigma_s}. \tag{4}$$

Developing a theoretical basis to identify the pore-scale capacitance based on geochemical and mineralogical considerations is the focus of ongoing research at PNNL and elsewhere. For example, under the PNNL Agile INSITE investment, the model of Bucker et al. (2019) is being used to define effective parameters at the scale of single pores. This model is being extended to 3D and will be deployed on HPC platforms. In the absence of such a tool, Maineult et al. (2017, 2019) assumed values for the relaxation time scales of pore-network bonds based on the assumption of effective diffusive length scales. We adopt a similar, heuristic approach here and assume values that reproduce realistic spectra. The pore-scale relaxation time associated with Equation (2) is (Dias, 2000):

$$\tau = C_s\left(R_f + R_s\right). \tag{5}$$

In future applications of the new model, the pore-scale capacitance could be defined using theoretical or experimental results from the tool developed under INSITE.

SIP spectra can be calculated efficiently by solving a Kirchoff AC circuit problem for the pore network; this involves construction of a system of conservation equations for electrical current. The pore-pore AC currents are simply $I=\Delta V/Z$ where is I current, ΔV is the potential difference between two pores, and Z is the impedance for the bond connecting the two pores, per Equations (2-4). Boundary conditions define specified potential along two sides of the model domain, to simulate current electrodes, and zero-current boundary conditions are assigned to other sides (Figure 3). The applied voltage is a complex quantity, with angular frequency ω and amplitude A. The amplitude is arbitrary and has no effect on the conductivity (or resistivity) spectra but is set equal to 1 mA. The electrical problem can thus be described by the linear system of conservation equations:

$$\boldsymbol{G}\boldsymbol{v} = \boldsymbol{b}, \tag{6}$$

where,

$\boldsymbol{G}$ is an admittance matrix, with complex-valued elements $\boldsymbol{G_{i,j}}$ equal to the inverse of the impedance of the bond connecting pores i and j;

$\boldsymbol{b}$ is a vector with elements equal to 0 for interior pores where current entering and exiting the pore remains within the network, and equal to boundary sources/sinks on model sides; these complex-valued currents are calculated based on the admittance to the boundary and boundary potential; and

$\boldsymbol{v}$ is a vector containing the complex-valued electrical potentials at every pore in the network.

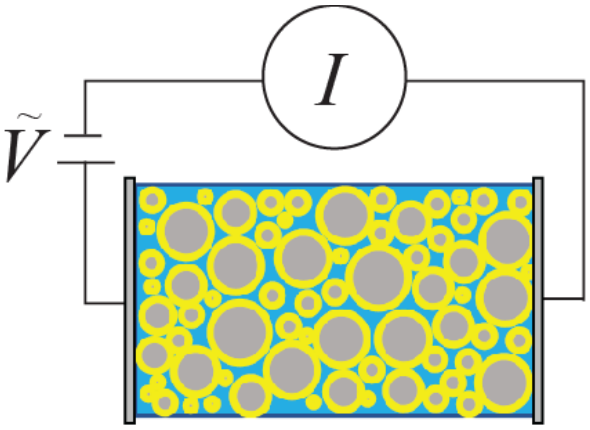

Figure 3. Schematic diagram showing the experimental analog to the pore network simulation, in which specific potential boundaries simulate electrodes at either end of a sample across which current is calculated.

In this work, a direct solver is used to solve Equation (6) for $\boldsymbol{v}$, but iterative and parallelized solvers could be used for modeling much larger systems. Solution of models on the scale of cores should be tractable on high performance computing platforms. $\boldsymbol{G}$ is very sparse having a number of non-zero elements equal to the number of pores times the average coordination number, which is 6 for a regular 3D cubic lattice.

Assuming sinusoidal steady-state conditions—an assumption consistent with SIP data acquisition—the SIP spectra can be calculated very efficiently. The amplitude or magnitude is given by:

$$\boldsymbol{A}(\boldsymbol{\omega}) = \left|\frac{\boldsymbol{I}_{\mathbf{boundary}}\, L_{\mathrm{total}}}{\boldsymbol{v} A_{\mathrm{total}}}\right|, \tag{7}$$

where A_{total} is the cross-sectional area of either the input or output boundary, $\boldsymbol{I}_{\mathbf{boundary}}$ is the current going through that boundary, and L_{total} is the distance between the two boundaries. The phase is given by

$$\boldsymbol{\varphi}(\boldsymbol{\omega}) = \boldsymbol{angle}\left(-\frac{\boldsymbol{I}_{\mathbf{boundary}}\, L_{\mathrm{total}}}{\boldsymbol{v} A_{\mathrm{total}}}\right). \tag{8}$$

Equations (7-8) calculates the spectra for the network based on the applied voltage and simulated currents observed at the two specified-voltage boundaries of the network. Experimentally, this is analogous to setting sinusoidal voltage at two electrodes on either end of a sample cell and measuring the magnitude and phase of the resulting sinusoidal current through the sample.

4.0 Results

The pore network model is demonstrated using a suite of synthetic examples for regular 3D cubic lattices (Figure 4). Whereas Maineult et al. (2017) observed 'huge' computation times and memory overflow problems for 2D lattice networks (4 bonds per pore) and only 10,000 pores, we see computation times <1 minute on a laptop for larger 3D problems, while sweeping over 30 frequencies. We attribute this improvement in computational efficiency to use of a different solution technique and sparse matrix operations that do not require QR factorization, the associated expansion of the system of equations, and the memory requirements to store full matrices.

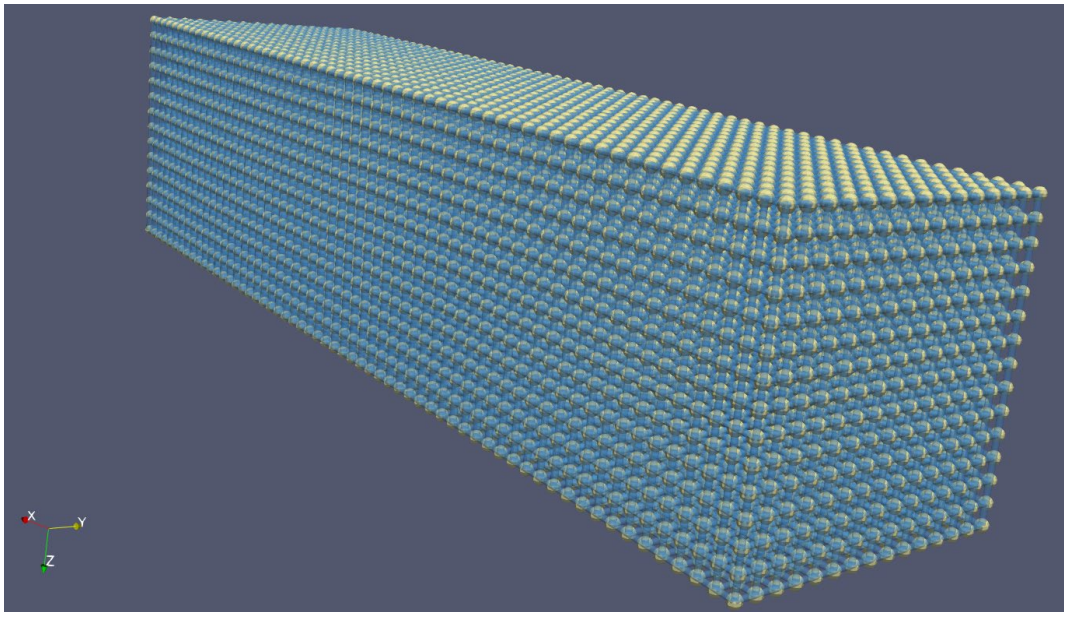

Figure 4. Regular cubic-lattice pore network with nx=60 and ny=nz=15 pores used in Example 1. Note that pore bodies and bonds are not drawn to scale.

The cubic lattice spans 60 pores in the x direction and 15 in each of the y and z directions. Other model specifications for the examples are detailed in Table 1. In the first example, we illustrate the role of C_s on the simulated spectra. As seen in Figure 5, varying this parameter shifts the phase response in frequency but does not affect the magnitude response. In the second example, we consider the role of surface conductance, Σ_s, which affects the magnitude response at high frequency and changes the phase response values in the absence of a frequency shift. In the third example, we vary the radius of the bonds between pores, R_{pipe}, which affects the conductance through the network and also changes the porosity; this changes the magnitude response and the values but shifts neither in frequency. In the fourth example, we vary the fluid conductivity, σ_f, which affects the magnitude response and phase but shifts neither in frequency.

Table 1. Model specifications for the examples.

Example	Coordination number	σ_f (S/m)	Σ_s (S)	R_{pipe} (μm)	L_{pipe} (μm)	C_s	Porosity (%)
1	6	0.04	2.5E-9	4	25	15, 10, 5	16
2	6	0.04	2.5E-9, 2.0E-9	4	25	10	16
3	6	0.04	2.5E-9	3.5, 4	25	10	12, 16
4	6	0.035, 0.04	2.5E-9	4	25	10	16

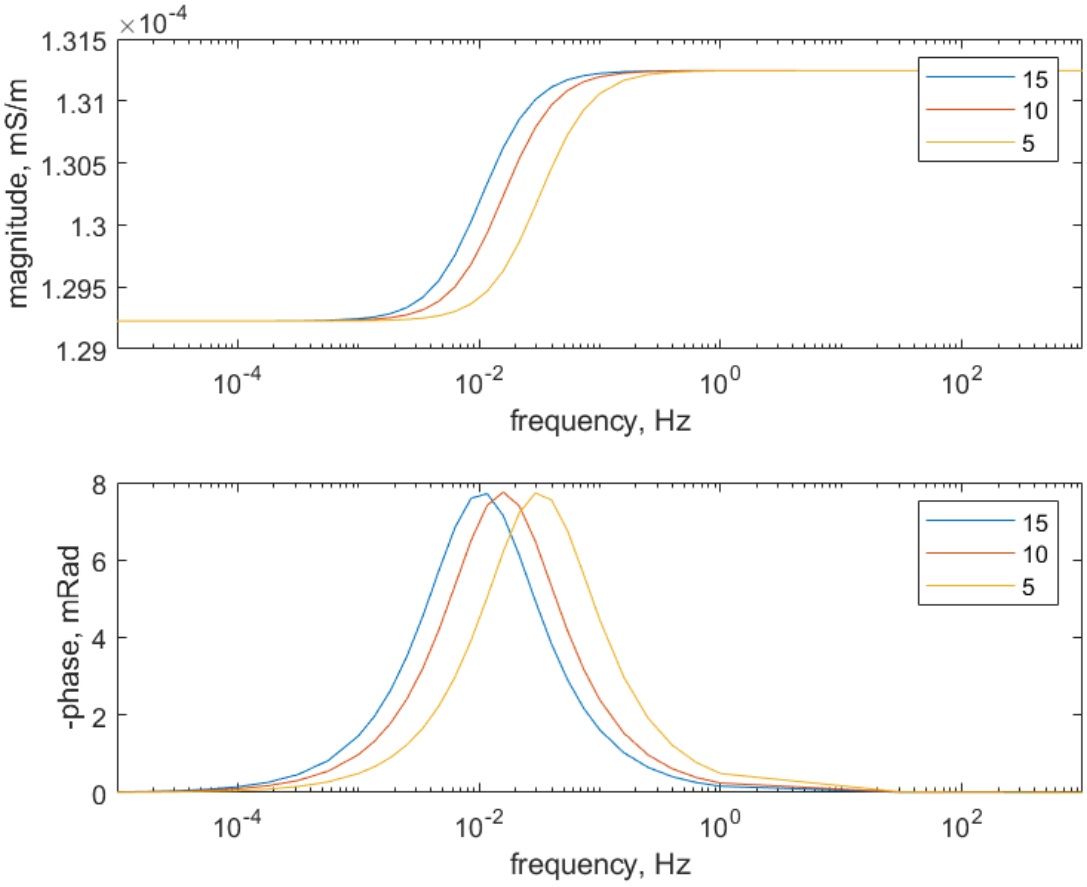

Figure 5. SIP response for Example 1, varying the value of C_s.

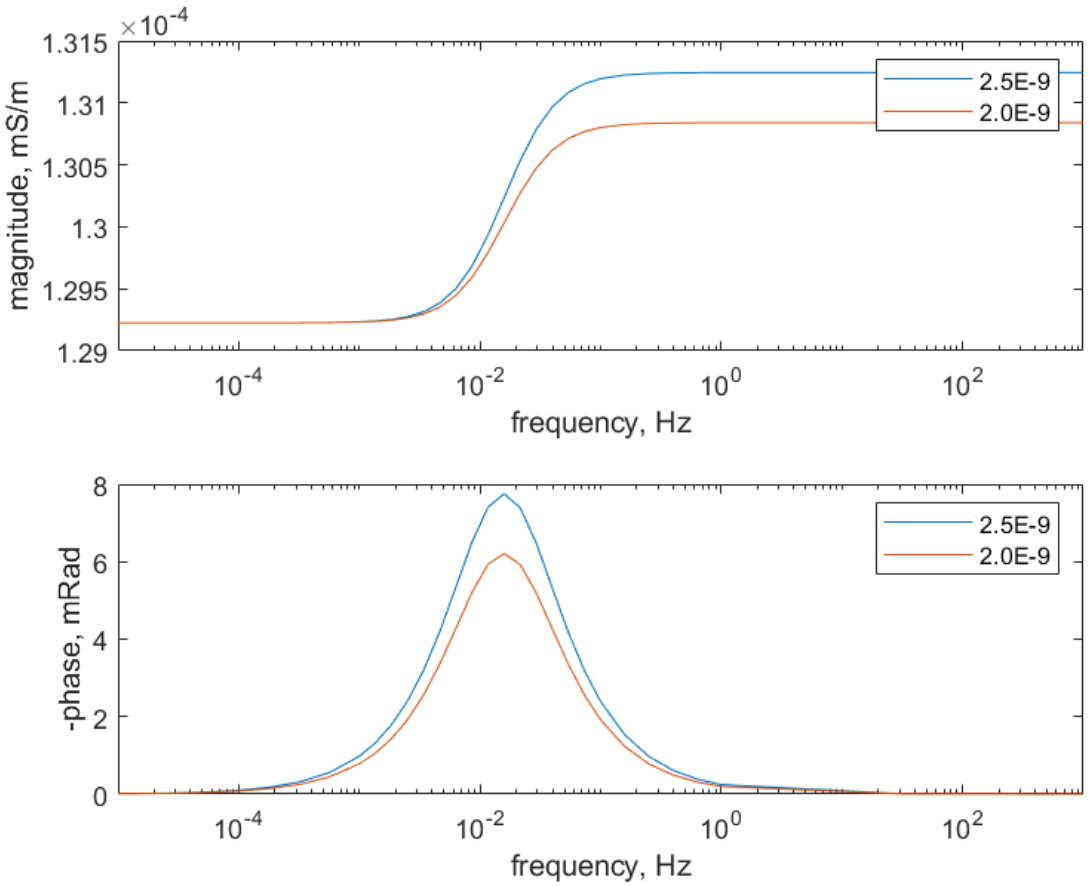

Figure 6. SIP response for Example 2, varying the value of Σ_s.

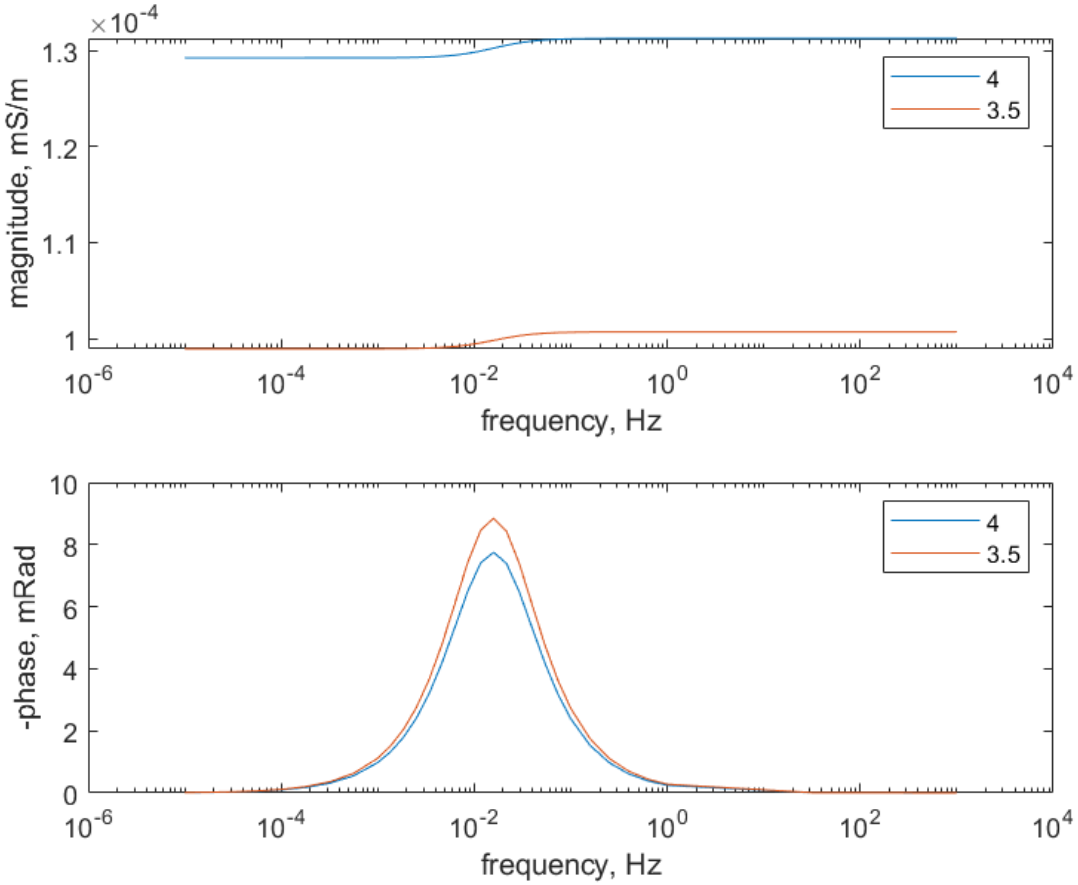

Figure 7. SIP response for Example 3, varying the value of R_{pipe}.

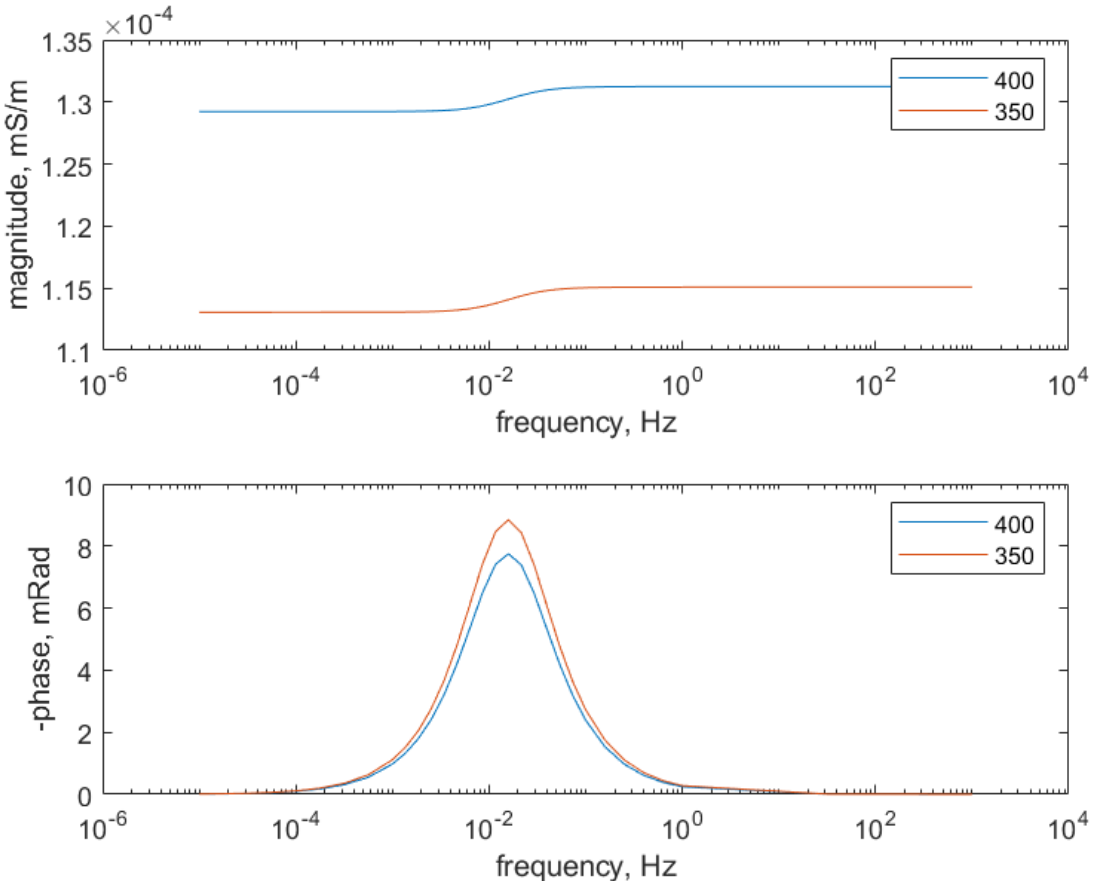

Figure 8. SIP response for Example 4, varying the value of σ_b

5.0 Discussion and conclusions

The pore network simulation results are consistent with expected behavior from previous work. The resistances of the two pathways, which are controlled by fluid conductivity, surface conductance, and pore geometry, affect the magnitude response and only the values of the phase response. Changing the surface conductance does not affect the magnitude response at low frequency, where the capacitance of the surface impedes conduction through that pathway. The capacitance associated with the surface pathway shifts the phase response in frequency. The model was tested and demonstrated on simple cubic-lattice networks but can simulate more complex networks.

The model presented is not as rigorous in its representation of pore-scale polarization as the model of Bucket et al. (2019); however, it is more computationally efficient and allows for simulation of much larger, 3D domains. Indeed, given the linearity of the problem, it should be possible to use linear model order reduction to build highly efficient simulators for large experimental cells, i.e., column scale.

The code was prototyped in Matlab but could be migrated to Python or FORTRAN to capitalize on high performance computing capabilities and parallelized solvers (e.g., petsc). Moving the code to Python would also allow better integration with the OpenPMN library for network generation (Gostick et al., 2016) and tools for network construction based on micro imaging (Gostick et al., 2019). Additional simulation capabilities in OpenPNM for flow and transport could also be leveraged to simulate coupled processes.

6.0 References

Bernabé, Y., M. Li, and A. Maineult, 2010, Permeability and pore connectivity: A new model based on network simulations, J. Geophys. Res.,115, B10203, doi:10.1029/2010JB007444.

Bernabé, Y., M. Zamora, M. Li, A. Maineult, and Y. B. Tang, 2011, Pore connectivity, permeability and electrical formation factor: A new model and comparison to experimental data, J. Geophys. Res., 116, B11204, doi:10.1029/2011JB008543.

Bernabé, Y., 1995, The transport properties of networks of cracks and pores, J. Geophys. Res., 100(B3), 4231–4241, doi:10.1029/94JB02986.

Blunt, M. J., 2001, Flow in porous media – pore-network models and multiphase flow, Curr. Opin. Colloid Interface Sci., 6, 197–2007.

Bücker, M., Flores Orozco, A., Undorf, S., & Kemna, A., 2019, On the role of Stern- and diffuse-layer polarization mechanisms in porous media. Journal of Geophysical Research: Solid Earth, 124, 5656–5677. https://doi.org/10.1029/2019JB017679

Day-Lewis, F. D., N. Linde, R. Haggerty, K. Singha, and M. A. Briggs, 2017, Pore network modeling of the electrical signature of solute transport in dual domain media, Geophys. Res. Lett., 44, 4908–4916, doi:10.1002/2017GL073326.

Dias, C., 2000, Developments in a model to describe low-frequency electrical polarization of rocks, Geophysics, 65 (2), 437-451.

Falzone, S., Slater, L., Schaefer, C., Keating, K., Caro, C., and Rodriguez, K., 2020, Could Emerging Geophysical Technologies Characterize PFAS Contamination in Source Zones?, Fast Times 25, no. 2, p. 41-47.

Gostick J, Aghighi M, Hinebaugh J, Tranter T, Hoeh MA, Day H, Spellacy B, Sharqawy MH, Bazylak A, Burns A, Lehnert W., 20016, OpenPNM: a pore network modeling package, Computing in Science & Engineering, 2016 May 25;18(4):60-74. doi:10.1109/MCSE.2016.49.

Gostick J, Khan ZA, Tranter TG, Kok MDR, Agnaou M, Sadeghi MA, Jervis R., 2019, PoreSpy: A Python Toolkit for Quantitative Analysis of Porous Media Images. Journal of Open Source Software, doi:10.21105/joss.01296

Greenberg, R. J., and Brace, W. F., 1969, Archie's law for rocks modeled by simple networks, J. Geophys. Res., 74(8), 2099– 2102, doi:10.1029/JB074i008p02099.

Kemna, A., Binley, A., Cassiani, G., Niederleithinger, E., Revil, A., Slater, L., Williams, K.H., Orozco, A.F., Haegel, F.-H., Hördt, A., Kruschwitz, S., Leroux, V., Titov, K. and Zimmermann, E., 2012, An overview of the spectral induced polarization method for near-surface applications. Near Surface Geophysics, 10: 453-468. https://doi.org/10.3997/1873-0604.2012027

Leroy, P., and A. Revil, 2004, A triple-layer model of the surface electrochemical properties of clay minerals, J. Colloid Interface Sci., 270,371–380.

Leroy, P., Revil, A., Kemna, A., Cosenza, P. & Ghorbani, A., 2008, Complex conductivity of water-saturated packs of glass beads, J. Colloid Interface Sci., 321(1), 103–117.

Lesmes, D. P., and Frye, K. M., 2001, Influence of pore fluid chemistry on the complex conductivity and induced polarization responses of Berea sandstone, J. Geophys. Res., 106(B3), 4079– 4090, doi:10.1029/2000JB900392.

Maineult, A., Revil, A., Camerlynck, C., Florsch, N., and Titov, K., 2017, Upscaling of spectral induced polarization response using random tube networks, Geophys. J. Int. 209, 948-960, doi:10.1093/gji/ggx066.

Maineult, A., Jougnot, D., and Revil, A., 2018, Variations of petrophysical properties and spectral induced polarization in response to drainage and imbibition: a study on a correlated random tube network, Geophys. J. Int. 212, 1398–1411 doi: 10.1093/gji/ggx474

Robinson, J., Slater, L., Weller, A., Keating, K., Robinson, T., Rose, C., et al., 2018, On permeability prediction from complex conductivity measurements using polarization magnitude and relaxation time. Water Resources Research, 54, 3436– 3452. https://doi.org/10.1002/2017WR022034

K. Singha, F. D. Day-Lewis, T. Johnson, and L. D. Slater. 2015. Advances in Interpretation of Subsurface Processes with Time-Lapse Electrical Imaging. Hydrological Processes, Hydrological Processes, 29(6):1549–1576.

Swanson, R. D., A. Binley, K. Keating, S. France, G. Osterman, F. D. Day-Lewis, and K. Singha 2015, Anomalous solute transport in saturated porous media: Relating transport model parameters to electrical and nuclear magnetic resonance properties, Water Resour. Res., 51, 1264–1283, doi:10.1002/2014WR015284.

Weller, A., and Slater, L.D., 2022, Ambiguity in induced polarization time constants and the advantage of the Pelton model, Geophysics 87 (6), https://doi.org/10.1190/geo2022-0158.1

Pacific Northwest National Laboratory

902 Battelle Boulevard
P.O. Box 999
Richland, WA 99354

1-888-375-PNNL (7665)

www.pnnl.gov